1988

Designing for Cantilevered Bearing Loads: Approach to Scroll Design

William R. Lane
Carrier Corporation - United Technologies

James S. Laub
Carrier Corporation - United Technologies

DESIGNING FOR CANTILEVERED BEARING LOADS: APPROACH TO SCROLL DESIGN

William R. Lane
Carrier Corporation
United Technologies
Syracuse, New York 13221

James S. Laub
Carrier Corporation
United Technologies
Syracuse, New York 13221

ABSTRACT

A method of accounting for the effect of cantilevered loading in the journal bearing design approach for scroll compressors is presented. An empirically derived edge loading factor is developed using a unique bearing test facility which can equate bearing system stiffness with load carrying capability. The edge loading factor is used to superimpose the cantilevered loading effects on a standard hydrodynamic film prediction program. This allows for complete analytic development of successful scroll journal bearing systems.

NOMENCLATURE

Symbol		Dimension
L	Bearing length	$[L]$
D	Bearing diameter	$[L]$
R	Journal radius	$[L]$
C	Radial bearing clearance	$[L]$
L_e	Effective bearing length	$[L]$
L^*	Dimensionless edge loading factor	$[-]$
V	Instantaneous eccentricity velocity	$[LT^{-1}]$
U	Linear journal velocity	$[LT^{-1}]$
p	Film pressure	$[FL^{-2}]$
μ	Film viscosity	$[FL^{-2}T]$
h	Film thickness	$[L]$
W	Bearing load	$[F]$
e	Journal eccentricity	$[L]$
ε	Dimensionless journal eccentricity	$[-]$
ω	Journal angular velocity	$[T^{-1}]$
ψ	Journal attitude angle	$[-]$
$\dot{\phi}$	Journal precession rate	$[T^{-1}]$
θ	Circumferential coordinate	$[-]$
t	Time	$[T]$
K_T	Bearing system stiffness	$[FL^{-1}]$
K_s	Shaft stiffness	$[FL^{-1}]$
K_b	Bearing component stiffness	$[FL^{-1}]$

INTRODUCTION

Scroll compressors pose an unique challenge for the compressor designer: predicting and designing for the effect of cantilevered shaft and bearing loading inherent in scroll geometries. A simple solution might be to incorporate rolling element bearings into the design to reduce the impact of edge loading. However, in the capacity ranges where scrolls are targeted for use, a rolling element bearing design might not be a cost effective alternative. The designer needs to develop a means of evaluating journal bearings which may operate with significant edge loading. Typical design tools such as computer simulations which predict bearing loads and calculate hydrodynamic film values do not accommodate the loss of effective bearing length resulting from edge loading. They also do not provide for

any means of incorporating bearing and shaft stiffness, which tend to affect the severity of edge loading, into the model. This paper presents a method by which empirically derived data provides a correlation between bearing system stiffness and an edge loading factor. The edge loading factor can account for the potential loss of available loading area in the bearing due to edge loading and be used to predict journal motion characteristics for any bearing design, given that the bearing system stiffness is known. The analysis can be accomplished using conventional computer simulations which predict hydrodynamic bearing performance. Therefore, cost effective scroll compressor bearing systems can be analytically designed and evaluated. Additionally, this method eliminates reliance on trial and error testing for achieving compatible shaft and bearing stiffnesses and subsequent reductions in bearing size and mass.

THEORY

While it is not the intention of this paper to redevelop the basis for hydrodynamic bearing theory, it is important that the factors which affect the successful operation of the dynamically loaded journal bearing be considered. The hydrodynamic bearing theories are derived from the general form of Reynold's equations for dynamic loading.

$$\frac{\partial}{\partial x}\left(\frac{h^3}{\mu}\frac{\partial p}{\partial x}\right) + \frac{\partial}{\partial z}\left(\frac{h^3}{\mu}\frac{\partial p}{\partial z}\right) = 6U\frac{\partial h}{\partial x} + 6h\frac{\partial U}{\partial x} + 12V_o \qquad (1)$$

The left hand side of equation (1) represents the contour of the hydrodynamic film in the x and z axis for a flat plate. The right hand side represents the forces which contribute to develop the oil film in the x-axis; the linear journal velocity (U), the precessive squeeze factor $\partial/\partial x$ and the radial velocity component (V_o) of the journal center itself. Conceptually the film generating forces are the same, but for the true journal bearing the equation reduces to the polar form.

$$\frac{1}{R^2}\frac{\partial}{\partial\theta}\left(h^3\frac{\partial p}{\partial\theta}\right) + h^3\frac{\partial^2 p}{\partial z^2} = 6\mu(\omega - 2\dot{\phi})\frac{\partial h}{\partial\theta} + 2\frac{\partial h}{\partial t} \qquad (2)$$

For a standard journal bearing, Figures 1 and 2 show that the shaft is aligned in parallel with the sleeve along the z-axis with a hydrodynamic film generated in the radial or x-axis supporting the applied load (W). Using this model and equation (1), prediction of the hydrodynamic film thicknesses and pressures is possible with sophisticated numerical analysis. Further refinements of the general Reynolds equations result in the finite length bearing solutions which incorporate end leakage effects. In particular, short bearing theory provides for relatively simple computational methods of predicting the eccentricity or motion of the journal within the bearing. From Reynold's equation (Eqn. 2), the developed hydrodynamic film becomes a function of the following shaft and bearing parameters.

$$h(\theta) = f(\mu, D, \omega, L, C, W) \qquad (3)$$

(Note: factors such as microfinish and manufacturing treatment of the bearing surfaces can have a significant effect as well, but these will not be considered for the purposes of the paper.)

To facilitate the evaluation, a Fortran based program utilizing short bearing theory and a simplified method of numerical analysis can be used to predict the behavior of a journal bearing system once the geometry and loading values are defined. Loading values for a scroll compressor can be obtained through use of a program such as the one introduced in Reference 1, whereby a scroll and bearing geometry is input and the calculated gas loads generate the resulting bearing loads. Other variables such as viscosity, shaft speed, bearing geometry and clearances are known and can be input as well. The predicted hydrodynamic film pressures, thicknesses and eccentricities can be used as guidelines for an acceptable bearing design, understanding that the model does not account for cantilevered loading of the shaft. Based upon past hydrodynamic bearing studies (Ref. 2,3), predicted eccentricity values (ε) in excess of 0.8 indicate that the system is nearing the point of film breakdown. Therefore, predicted eccentricity values (ε) below 0.6, for example, would be desirable.

Though the program has demonstrated good correlation with other, more sophisticated, methods of hydrodynamic film prediction, a problem with using predicted values for design guidelines is that the model presumes that the shaft load is supported over the entire bearing length (L). The model also assumes that the loading is applied in a simply supported manner. For rotary and reciprocating compressor designs, when the gas forces are between the bearings, these assumptions are acceptable. For the scroll, however, cantilevered gas loading can lead to edge loading effects. Therefore, in addition to the parameters described in Eqn. 3 which define the hydrodynamic film thickness (h_0), the stiffness of the bearings and shaft (K_s, K_T, K_b) must also be considered factors in the load carrying capability of the bearing. This fact is no surprise to compressor designers. Typically, in the course of designing an effective journal bearing system, some adjustments are made to the stiffness of either the shaft or the bearings in response to evidence of edge loading. However, bearing systems which are designed with low stiffnesses to alleviate edge loading effects can create other problems such as air gap instability or excessive shaft whip. It may therefore be necessary to maintain a certain level of bearing system rigidity though it can contribute to the likelihood of edge loading.

In operation, edge loading manifests itself as wear patterns on small bands near the end of the bearings. This means that the entire shaft load is carried by an oil film which is developed over a much smaller region of the shaft (Fig. 3) than is considered in the bearing models. In many cases, this effective bearing length can be substantially smaller than the presumed load carrying length (L). Therefore it is desirable to be able to model this condition for prediction of journal motion. However, for the model to work, simply supported loading must still be assumed and the hydrodynamic film will be predicted for the length of the bearing input to the program. It seems then, that modelling the edge loaded shaft as a two land bearing with land lengths equivalent to the supported region in the edge loaded condition is a reasonable assumption (Fig. 4). The true effective bearing length (L_e) can be used within the short bearing model as the land length for a two land bearing to predict journal eccentricity for the actual gas loading values incorporating the effects of the varying shaft and bearing stiffnesses. The difficulty in utilizing this approach is in determining the actual L_e values for each bearing.

The use of a bearing test vehicle which applies a controlled load to the shaft system and monitors bearing response to the load could provide a relationship between shaft and bearing stiffnesses and edge load effect. Such a test vehicle is described in the Experimental Program section. This information allows for derivation of a non-dimensional edge load factor, L^*, which represents the percent of available bearing surface which is used to support the shaft loading.

$$L^* = L_e/L \qquad (4)$$

$$L^* = f(\mu, D, \omega, L, C, W, K_T, K_s, K_b) \qquad (5)$$

L^*, then, is clearly related to the parameters which define the hydrodynamic film thickness as well as the accompanying bearing and shaft stiffnesses. Since the hydrodynamic prediction program can account for the parameters which define h_0, the edge load factor reduces to a function of the stiffnesses. That is, L^* is related to the overall stiffness of the bearing system (K_T), shaft (K_s) and the stiffness of the bearing (K_b) under evaluation.

$$L^* = f(K_T, K_s, K_b) \qquad (6)$$

L^* is empirically derived by correlating the actual load to failure values from the test vehicle for a particular system with the L_e value required to force predicted journal eccentricity to exceed 0.8 for that same system geometry. Through test evaluation of different geometry and stiffness bearing systems, a relationship can be developed between load to failure and stiffness. The loading values can be plugged into the prediction program, along with the appropriate geometries, to determine eccentricity. For each loading value, progressively smaller values of L_e are used until the predicted eccentricity surpasses 0.8. This establishes the L_e value for that particular geometry and consequently the L^*. Because L^* is dimensionless, it can be plotted directly against the stiffness for each individual bearing system. When a group of bearing system results are plotted, a curve results which now describes L^* for any system stiffness (Fig. 5).

Thus, once the stiffness is known for a bearing system and its components, the edge loading factor can be determined. If the eccentricity predicted for the system is under 0.6 for the anticipated gas loading at a maximum loading condition (Reference 1), then the bearing system should be acceptable under operation. Stiffnesses for the components can be established using empirical testing or analytical tools such as finite element analysis or simple static models. The system stiffness can usually be predicted within ten percent of actual values.

EXPERIMENTAL PROGRAM

The Carrier bearing tester is used to develop the relationship between L^* and K. This unique apparatus has typically been used to perform comparative tests on various compressor bearing components. This is the first time it has been used specifically in design qualification. The bearing tester provides the capability to study practically all aspects of journal bearing performance. Such capability can be extremely valuable in reducing design evaluation time, study of bearing details, and evaluating alternate materials and processes.

Testing machine description

The Carrier bearing test machine is composed of a closed loop servo hydraulic materials test machine. A pressure vessel test chamber contains the test specimen; this assembly is supported by a hydraulic load frame. A separate lubrication system is plumbed into the test chamber. Various temperature, torque and fluid flow measurement systems are accessory to the machine.

The heart of the test apparatus is the test chamber, incorporating a mounting plate for holding a bearing pedestal when tests are performed on bearing and journal couples. Complete crankcases can be supported on appropriate mounting brackets. A scroll crankcase was used for the tests in the present discussion, see Figure 7 for a schematic of the test configuration.

A quill shaft is used to rotate the compressor test shaft. It is belt driven externally by an electric motor. Changing bearing rotation speeds is a simple matter of changing pulleys on the motor and quill shaft. A hydraulic ram with a servo valve is used to provide programmed test loads to the test bearing system. Separate shaft torque transducer sections are incorporated in the shaft drive line for torque measurements. The servo hydraulic system provides for static, monotonic increasing, dynamic and changing dynamic radial loads on the bearings. Cycling can be controlled by load, ram stroke, or strain. Loading frequencies keyed to shaft rotation are imposed with visually acceptable sine wave shape. The standard digital function generator can also supply triangular, sawtooth and square waves, but with the usual mechanical deterioration of the signals as the frequency increases. Cycle counting, end of cycle shutdown, and over and under peak detection circuits are provided for program control and monitoring.

Auxiliary circuit sensing of bearing temperatures via thermocouples provides test monitoring and termination at any preset bearing temperature. An X-Y-Y plotter and a digital oscilloscope are built into machine monitoring section. A load cell is used to measure the bearing applied loads. Various strain gage transducers can be incorporated into the tester as required.

A separate lubrication system is provided for the test bearings. This unit has pressure control, flow meters, and filters to provide a fully controlled lubrication stream to the test bearings. Incorporation of various proportions of refrigerant in the lubricant stream is possible. The pressure vessel test enclosure was designed to handle the full range of potential refrigerant pressures.

In the present configuration, a scroll crankcase is mounted via its normal mounting surface on a bracket, which in turn is attached to the tester mounting plate. The test bearings are in their fixed design locations. A dummy compressor shaft (which may be a modified scroll shaft) is held in a single spherical roller bearing attached to the hydraulic ram and supported by the bearings in the crankcase. A quill shaft is piloted an threaded into the scroll end of the shaft to provide rotation of the shaft in its bearings. The lubrication system feeds the compressor shaft through an oil gallery in the quill shaft, so that lubrication of the bearings is provided in the normal manner.

Scroll bearing tests

The scroll bearing tests reported here were the initial tests used to check and tentatively establish the loading and stiffness relationship. These tests included the determination of shaft and bearing mounting stiffnesses. This was done in the conventional manner by applying loads either directly to the bearing mountings or through a shaft into the bearings. The shaft stiffness was determined independently. Strain gaged displacement transducers used to monitor component movement were mounted so that fixturing compliance was eliminated from the measurements. Once the stiffnesses were determined and checked against calculated values, simulated compressor loading of the bearings was initiated.

Simulated compressor loading tests begin by establishing lubrication flow; the bearing load is zeroed and shaft rotation is started by energizing the quill drive motor. Bearing temperatures increase from ambient by friction and shear losses. This is monitored until the highest bearing temperature reaches a predetermined base level, at which temperature a monotonically increasing load is applied to the shaft at the scroll load line center at a constant rate (Fig. 8). The load and bearing temperatures are recorded on the integral X-Y-Y plotter. Some experience is required to locate the thermocouples at the most critical bearing locations; however, after the first ramp load to seizure test is completed, correct thermocouple locations are readily apparent from observation of the distressed areas.

Each test is started with a zero load warm up period, whose duration depends to some extent on the component geometries and fits. In all cases, enough time is provided so that a rotating bearing load vs. time signature at nominal zero load can be recorded on the storage oscilloscope. This record is used to evaluate the consistency of part fit-up and the assembly procedures. An experienced technician can easily check each step of the assembly procedure by the torque required to rotate the shaft in the assembly. During the warm up period, the X-Y-Y plotter records temperature of both bearings as a function of time. Once the loading cycle is started, the X axis on the plotter is switched over to a precalibrated load scale.

Figure 9 is an example of data obtained from the scroll bearing maximum load capacity checks. Once the highest temperature bearing, bearing A in this instance, reaches the base temperature under no load rotation, the monotonic loading ramp function is initiated. The data traces show a proportional increase in temperature with increasing load, until the lubrication film is broken and seizure occurs with an instantaneous increase in bearing temperature. By removing the load at the time of temperature increase, limited damage is done to the bearings. For this test, bearing A is the limiting component with lubricant film breakage and consequent seizure. At this point, the system may be disassembled and the bearing and shaft surfaces examined to determine the exact location and nature of the damage.

To date our testing has been aimed at qualification of the scroll bearing system against expected maximum radial loads and development of the optimum components stiffness and support locations within the geometric confines of the overall design. The bearing test machine has proven to be a uniquely valuable tool in these studies, and we believe it represents a significant advance in the experimental technical capability of the industry.

The bearing tester is extremely flexible, allowing such additional single variable studies as:

Bearing and shaft material static and dynamic strength
Bearing and shaft surface finish load carrying capacity
Lubricant film strength
Lubricant plus refrigerant film strength
Temperature effects on load carrying capacities
Loading speed and cycle shape effects on load capacity

RESULTS

Loading values established on the Carrier bearing tester for particular scroll bearing system geometries confirmed that edge loading is a consideration for scroll

bearing systems. First, visual evidence of edge loading was apparent upon examination of several failures. Second, the loading values which generated failures resulted in predicted eccentricities substantially lower than 0.8 for that particular bearing geometry using the full length (L). These results confirm that some type of factor is required to force the program to predict failures for loading values at which they occur. As proposed in the theory section, decreasing L^* values were chosen for the known failure loads and are shown in Figure 6. These eccentricity maps show that for $L^* = .10$, the program predicts bearing failure ($\varepsilon > 0.8$). This indicates that for this particular bearing/shaft stiffness, the edge loading area is on the order of 10% of the full bearing length.

The curve for L^* versus K_T (Fig. 5) will be further developed as other parameters, such as bearing surface treatment, are more extensively evaluated. However, the curve as currently established allows for complete analytical development of different bearing systems for cost reduction and new model development. Test results of various system stiffnesses have confirmed the L^* vs. K_T relationships. Certainly the efficiency of design has increased.

CONCLUSIONS

A method of analytically determining the effectiveness of a journal bearing lubrication system for scroll compressors was established. In addition, it was recognized that the standard methods for predicting hydrodynamic film response to shaft loading was inadequate for the cantilevered loading seen in scroll compressors. An empirical method was developed utilizing a unique bearing evaluation technique to derive a relationship between bearing and shaft stiffness and an edge loading factor. This relationship allows for the efficient use of a short bearing theory program to predict the eccentricity of a shaft journal which is loaded in a cantilevered manner. The criterion for success is that the resultant eccentricity (ε) must be <0.8. This process eliminates the tremendous reliance upon durability testing and failure analysis for preliminary design of new lubrication schemes for scroll compressors and is applicable to other compressor types as well. The bearing test equipment can be used to further validate stiffness and load carrying capability and also identify benefits associated with various surface treatments of the journals and bearings.

REFERENCES

1. Etemad, S., et al, "Computational Parametric Study of Scroll Compressors", Procedure of the 1988 International Compressor Engineering Conference (Purdue), July 1988.

2. Booker, J.F., "Design of Dynamically Loaded Journal Bearings", Fundamentals of the Design of Fluid Film Bearings, S.M. Rhode, et al, Book No. H00145, ASME, 1979, pp. 31-44.

3. Booker, J.F., "Dynamically Loaded Journal Bearings: Mobility Methods of Solution," Trans. ASME, Journal of Basic Engineering, Sept. 1965. pp. 537-546.

4. Pinkus, Oscar and Sternlight, Beno, Theory of Hydrodynamic Lubrication, Mcgraw-Hill, 1961.

5. Shaw, Milton and Macks, Fred, Analysis and Lubrication of Bearings, Mcgraw-Hill, 1949.

6. Fuller, Dudley, Theory and Practice of Lubrication for Engineers, John Wiley and Sons, Inc. 1956.

7. Lund, J.W. and Thomsen, K.K., "A Calculation Method and Data for the Dynamic Coefficients of Oil-Lubricated Journal Bearings", Topics in Fluid Film Bearing and Rotor Bearing System Design and Optimization, ASME, 1979, pp. 1-28.

8. Barrett, L.E., Allaire, P.E. and Gunter, E.J., "The Dynamic Analysis of Journal Bearings Using a Finite Length Correction for Short Bearing Theory", ibid., pp. 29-42.

FIGURES

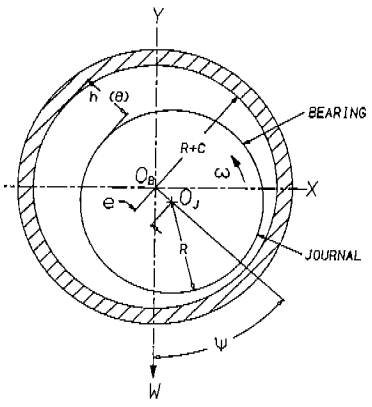

STANDARD BEARING JOURNAL
FIG 1

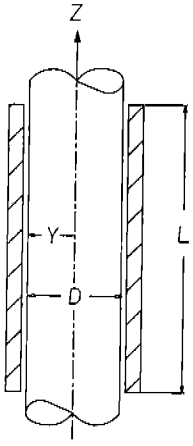

STANDARD JOURNAL BEARING
FIG 2

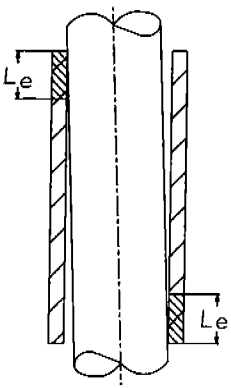

EDGE LOADING EFFECT

FIG 3

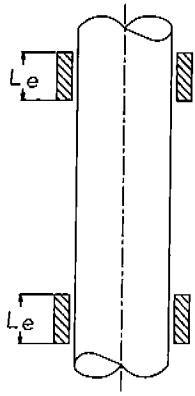

EDGE LOADING MODEL
(2 LAND BEARING)
FIG 4

EDGE LOADING FACTOR (L*)
VS SYSTEM STIFFNESS (K_T)

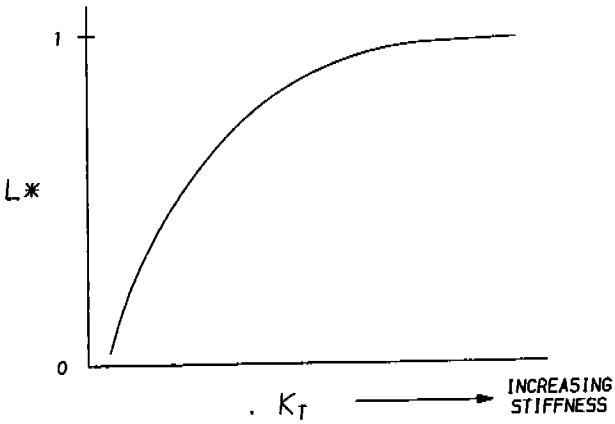

FIG 5

ECCENTRICITY VS. EDGE LOADING FACTOR (L*)
FOR EXPERIMENTAL LOAD OF FAILURE

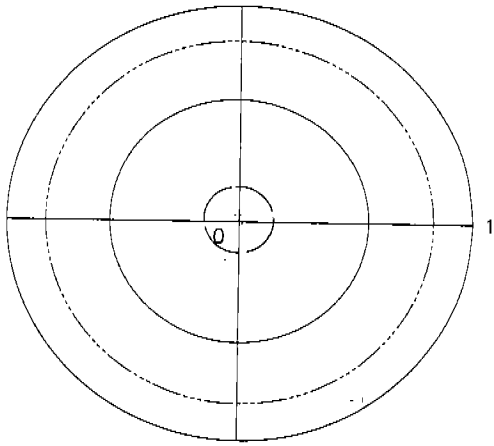

L* = 1
L* = 0.5
L* = 0.25
L* = 0.125
L* = 0.10

FIG 6

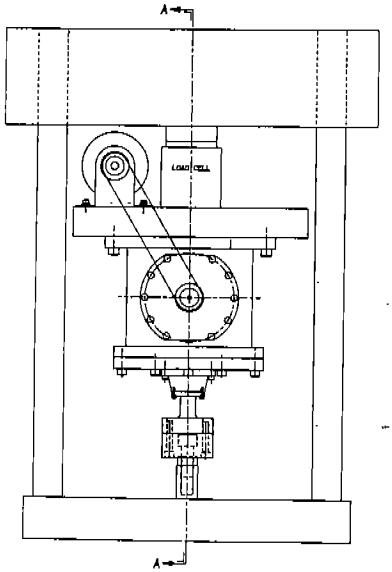

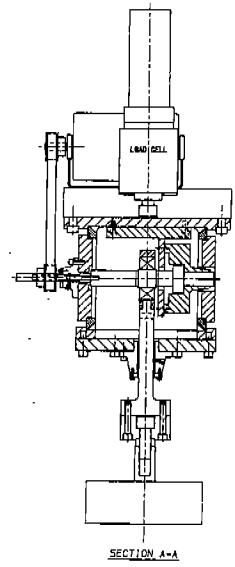

SECTION A-A

CARRIER BEARING TESTER
FIG 7

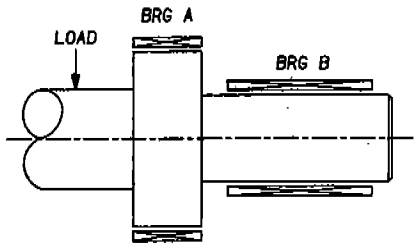

SHAFT LOADING
FIG 8

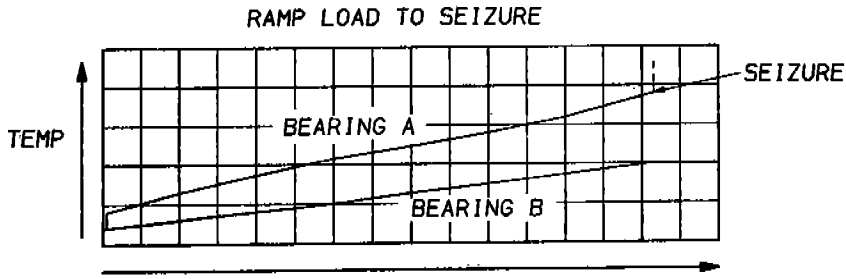

FIG 9